

Highly Ordered Noncrystalline Metallic Phase

Gabrielle G. Long,^{1,2,*} Karena W. Chapman,¹ Peter J. Chupas,¹ Leonid A. Bendersky,²
Lyle E. Levine,² Frédéric Mompou,^{2,3} Judith K. Stalick,⁴ and John W. Cahn^{2,5}

¹*X-Ray Science Division, Argonne National Laboratory, Argonne, Illinois 60439, USA*

²*Materials Science and Engineering Division, National Institute of Standards and Technology, Gaithersburg, Maryland 20899, USA*

³*Centre d'Élaboration de Matériaux et d'Études Structurales, CNRS, 31055 Toulouse, France*

⁴*NIST Center for Neutron Research, National Institute of Standards and Technology, Gaithersburg, Maryland 20899, USA*

⁵*Department of Physics and Astronomy, University of Washington, Seattle, Washington 98195, USA*

(Received 14 February 2013; published 2 July 2013)

We report the characterization of a unique metallic glass that, during rapid cooling of an Al-Fe-Si melt, forms by nucleation, followed by growth normal to a moving interface between the solid and melt with partitioning of the chemical elements. We determine experimentally that this is not a polycrystalline composite with nanometer-sized grains, and conclude that this may be a new kind of structure: an atomically ordered, isotropic, noncrystalline solid, possessing no long-range translational symmetry.

DOI: [10.1103/PhysRevLett.111.015502](https://doi.org/10.1103/PhysRevLett.111.015502)

PACS numbers: 61.43.Fs, 72.80.Ng

There are classes of ordered 3-dimensional (3D) arrangements of points that are neither periodic nor quasiperiodic [1]. We report the creation and structural analysis of a noncrystalline isotropic metallic solid that may be a material realization of such an arrangement. During rapid cooling of an Al-Fe-Si melt, this solid forms by means of nucleation, followed by growth of the solid into the melt. We observe evidence of chemical partitioning at the interface that, in multicomponent systems where freezing over temperature ranges spreads out latent heats and volume changes, is a convenient defining characteristic of first-order phase transitions. Such a transition allows composition changes and ordering to produce an optimal low-energy structure.

The microstructural evidence for this formation mechanism of the solid is shown in Fig. 1(a). The round features are the nodules of the noncrystalline isotropic solid [Figs. 1(b) and 1(c)], which are surrounded by radiating patterns of crystalline aluminum. Evidence that the solid is isotropic is presented below. Unlike the usual case of a glass that is formed on cooling to where atom motion ceases, and where the glass is the last phase to form, the nodules' central locations indicate that the solid glassy nodules were the first to solidify from the melt [2]. As in the case of crystals growing from solutions, the growing nodules deplete the surrounding melt, in this case of iron and silicon. When the melt is enriched enough in aluminum, it solidifies as the radiating pattern of aluminum crystals. In turn the growing aluminum crystals reject the melt's residual iron and silicon, which can be detected in the thin gray layers between the crystals.

More evidence of partitioning comes from the narrow (≈ 10 nm) white band of aluminum around each nodule. This arises from a diffusion zone in the melt that is more depleted of iron and silicon and enriched in rejected aluminum. Its thickness is approximately D/v , where D is a diffusion coefficient and v is the nodule interface growth

velocity. Assuming a typical liquid phase diffusion constant of $D \approx 10^{-9}$ m²/s implies that $v \approx 0.1$ m/s. With a fundamental frequency of 10^{13} /s, there can be about 10^4 attempts before a typical atom joins the solid. There is a diffusional instability associated with such diffusion zones [3], seen in Fig 1(a) as undulations in the interface. These observations, taken together, provide strong support that the formation mechanism is the normal and well-studied partitioning of a crystalline solid growing from a solution.

Formed by a first-order transition from the melt, this solid can also differ structurally from the melt. Because it is isotropic in high-resolution transmission electron microscopy [Fig. 1(b)] and electron diffraction [Fig. 1(c)], we have called it “ q glass” even though it is not a typical glass that is formed at a glass transition when atomic motion in a melt ceases. Additional evidence that the solid is isotropic comes from examination of the intensity distribution around the first x-ray diffraction ring; no anisotropy was observed.

Specimens that are 100% q glass [Fig. 1(d)] can be grown with a composition close to 15 at. % Fe, 20 at. % Si. To probe the atomic ordering of the q glass, we used the pair distribution function (PDF) method [4] to explore its local structure and investigate the relationship of the q glass to crystalline α -phase Al-Fe-Si [5,6] and icosahedral Al-Fe-Si, which are neighboring phases in the ternary phase diagram. The samples are listed in Table I.

High energy (80.725 keV, $\lambda = 0.15359$ Å) x-ray scattering data suitable for radial PDF analysis were collected at the Advanced Photon Source (APS), Argonne National Laboratory, beam line 11DC [7] from nearly single-phase samples of the α , icosahedral, and q -glass phases in the Al-Fe-Si system (See Table I). The PDF analysis made use of the diffraction data collected with a small (10×10 μ m) beam. Contributions to the scattering from the sample environment and background were subtracted. Corrections

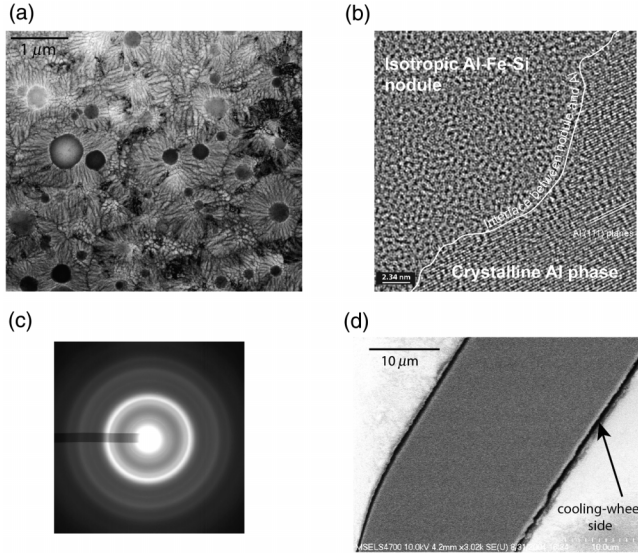


FIG. 1. Overview of the metallic alloy glass. (a) Microstructure of an $\text{Al}_{01}\text{Fe}_7\text{Si}_2$ alloy after electron beam surface melting with a scan velocity of 50 cm/s. The nodules at the center of radiating patterns of crystallization are glass. This morphology indicates that the glass was first to solidify from the melt. (b) High resolution TEM image near a nodule-Al interface showing isotropic nature of the nodule. (c) Electron diffraction from the nodule showing glasslike continuous diffuse rings. (d) SEM image of a cross section of a melt-spun ribbon of the Al-15Fe-20Si at. % alloy showing a uniform glassy structure throughout the thickness.

for multiple scattering, x-ray polarization, sample absorption, and Compton scattering were applied to the diffraction patterns to obtain the structure factor $S(Q)$, where Q is the magnitude of the scattering vector. Direct Fourier transform of the reduced structure function $F(Q) = Q[S(Q) - 1]$ up to $Q \approx 18 \text{ \AA}^{-1}$ gave the PDFs $G(r)$. Here, $G(r) = 4\pi r[\rho(r) - \rho_0]$, where $\rho(r)$ and ρ_0 are the instantaneous and average densities and r is the radial distance between atom pairs. The extraction of $G(r)$ and the structural refinement were conducted within the analysis software PDFFIT [4].

Particular care was required to fit quantitatively a structural model to the experimental PDF data. The α -cubic crystalline structure ($Pm\bar{3}$, $a \approx 12.5 \text{ \AA}$) is complex, with 138 atoms per unit cell on 11 Wyckoff positions. This is a large structure compared to structures typically refined using PDF methods. It was useful to compare the fit of the crystalline α -cubic phase model to the PDFs for each

sample, applying crystallographic symmetry constraints. Refinement of the structural model against the PDF data for α -cubic Al-Fe-Si, refining lattice parameter ($a = 12.55 \text{ \AA}$), atomic displacement parameters, and atomic positions within the symmetry constraints, yielded a reliable fit (with a weighted profile R factor, $R_{\text{wp}} = 13.9\%$) [8]. This fit [9] is comparable in quality to reported refinements of single crystal diffraction data, although the weighting of the PDF by a prefactor of Q (i.e., Fourier transform of $F(Q) = Q[S(Q) - 1]$), placing emphasis on high Q data, causes the numerical value of R_{wp} to be inflated relative to a Bragg refinement of equal quality. As crystalline Al may be within the scattering volume, we attempted to fit the experimental data with α -phase plus crystalline Al, but we found no significant Al inclusions in this sample. For comparison, the α -cubic Al-Fe-Si model refined against data from the icosahedral Al-Fe-Si phase yielded a less good fit ($R_{\text{wp}} = 28.5\%$, $a = 12.06 \text{ \AA}$). Refinement of a structural model for the α -cubic approximant phase against the PDF from the glass yielded an agreement factor of $R_{\text{wp}} = 22.3\%$, and a lattice parameter, $a = 12.26 \text{ \AA}$. This indicates that the motifs in the approximant are a better representation of the motifs in the glass than in the icosahedral phase.

Figure 2 shows the total PDF, $G(r)$, of all three phases overlaid for comparison. The data have been scaled (by $1.024r$) for the q glass and (by $1.041r$) for the icosahedral phase to improve the overlay of the general features of the PDFs and to account for the compositional-dependent mean atomic distances. In PDF analyses, these distances are referred to as refinement lattice parameters, shown in Table I, of the different phases.

Note that $G(r)$ from the q glass decreases in amplitude around 12 \AA , which indicates that the environments of the atoms in the q glass and the α -cubic phase (and the quasicrystalline phase) are similar out to that distance. For the α -cubic and icosahedral phases, this refers to the atoms in and between the underlying icosahedral clusters. Because $G(r)$ reflects pairwise-atom rather than multiatom correlations, we cannot determine what types of motifs the q glass shares with the crystal. We note that an ordering distance of 12 \AA is inconsistent with crystallinity because one cannot have translational invariance with a single cell.

Given the strong similarity between the structure of the α -Al-Fe-Si sample and the q glass, it is important to investigate the possibility of the q glass being a nanocrystalline or microcrystalline structure [10–12]. We consider a

TABLE I. List of samples and fitted lattice parameters.

Sample name	Phase	Composition (at. %)	Lattice parameter, a
α -AlFeSi	Crystalline α -cubic	Al-18Fe-8Si	12.55 \AA
ico-AlFeSi	Quasicrystalline icosahedral	Al-18Fe-22Si	12.06 \AA
q -AlFeSi	q glass	Al-15Fe-20Si	12.26 \AA

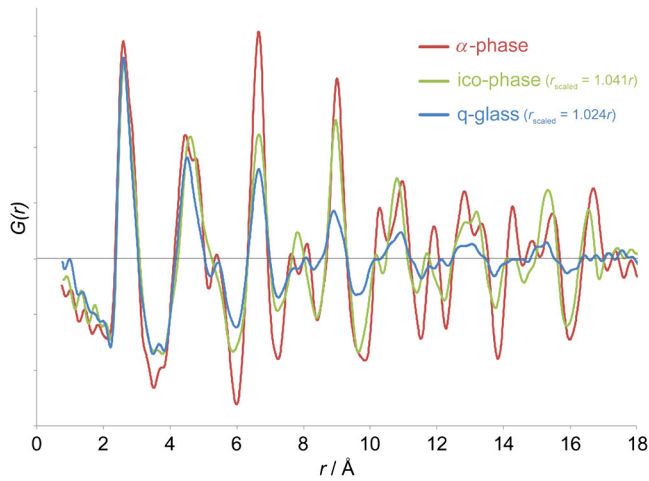


FIG. 2 (color online). $G(r)$ of the three phases overlaid for comparison. To improve the overlay of the general features of the PDFs and to account for the different lattice parameters of the different phases, the data have been scaled (by $1.024r$) for the glass and (by $1.041r$) for the icosahedral phase.

nano- or microcrystalline solid to be a material in which the grain structure coarsens upon annealing with no phase transition involved. To investigate this, we examined the evolution of the broad glassy diffraction peaks during an isothermal anneal. The grains of a nano- or microcrystalline solid would coarsen upon annealing, and corresponding diffraction data would show α -crystalline Bragg peaks

growing out from under the broad diffraction peaks of the glass with a narrowing of the broad peaks.

We followed the behavior of the q glass by monitoring the phase transformations [10,11] during isothermal annealing, using high energy (≈ 58 keV, $\lambda \approx 0.213$ Å) x-ray scattering data collected at beam line 11 ID B at the APS. The sample was mounted orthogonal to the (250×250) μm x-ray beam within a temperature controlled sample environment (DSC Thermatica System) from Linkam Scientific Instruments (Any mention of commercial products is for information only; it does not imply recommendation or endorsement by NIST). Data were collected at ambient temperature, and during annealing of the q glass at 330°C (3 h) and 305°C (16 h). During the *in situ* synchrotron x-ray diffraction measurements through the 330°C isothermal anneal, the q glass persisted for about 40 min with no measurable change in the diffraction, after which it transformed *via* a first-order phase transition to β - $\text{Al}_{4.5}\text{FeSi}$ [13]. The β - $\text{Al}_{4.5}\text{FeSi}$ structure is a monoclinic phase with no icosahedral motifs. Some β -phase peaks appear between the broad glassy peaks.

During an extended isothermal anneal at 305°C (see Fig. 3), there was clear diffraction evidence of face-centered cubic (fcc) Al in the early *in situ* data. By following the growth of the intensity of the crystalline Al diffraction peaks as a function of time, we discovered that q glass precipitates excess aluminum at this temperature. The peak widths showed no indication of a relaxation to a

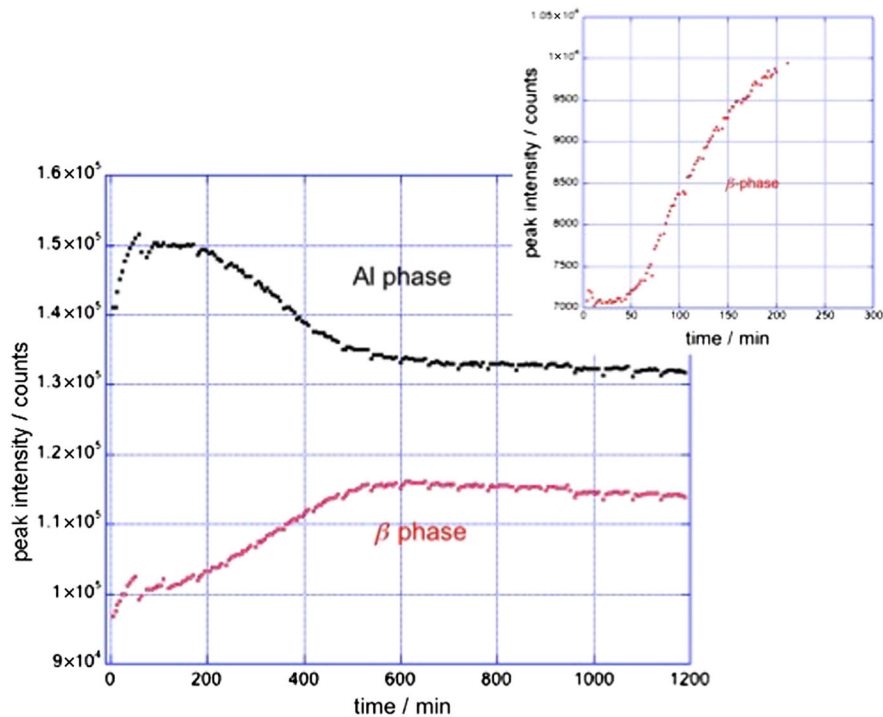


FIG. 3 (color online). Peak intensities from the crystalline phases as a function of time during the 305°C and (inset) 330°C thermal anneals show the increase of the β phase and increase and later decrease in the fcc Al phase at 305°C . As a result of a declining x-ray beam intensity, the plateaus that start at 600 min. are actually flat and indicate that equilibrium has been reached.

more stable q glass. After the q glass rejects Al, this two-phase mixture persisted for approximately an hour until a new phase, β -Al_{4.5}FeSi, grew in, consuming both the remaining q glass and most, but not all, of the fcc Al. Without the excess Al, it would have been difficult for the β -Al_{4.5}FeSi to form and grow. This is a classic peritectoid reaction in which two phases, in our case the fcc Al and the q glass, react to form another phase, the β -Al_{4.5}FeSi. Analysis of the annealed product by means of Rietveld refinement of the diffraction pattern indicates that the product is 90 wt. % β -Al_{4.5}FeSi and 10 wt. % fcc Al.

In contrast, an isothermal anneal at 330 °C showed no precipitation of fcc Al (Fig. 3 inset), although there was again no indication of a relaxation to a more stable q glass. However, the product is the same as that of the lower temperature anneal: namely a β -Al_{4.5}FeSi phase that incorporates more aluminum. We conclude that the q glass acts as an ordinary solid phase with a larger compositional stability range at the higher temperature.

During the *in situ* anneals, we found that the broad x-ray diffraction rings from the q glass remained broad and gradually diminished in intensity while sharp diffraction peaks from the unrelated β -Al_{4.5}FeSi crystalline phase appeared and grew. This is consistent with the transition of a phase that is in metastable equilibrium and remains unchanged until transformed in a first-order transition.

From the above observations, we conclude that the q glass is a highly ordered isotropic phase that is in metastable equilibrium and certainly is not a polycrystalline aggregate of nanometer-sized crystalline grains. This leads us to expect that the energy and entropy of the q glass are comparable to that of a crystal or quasicrystal. Because it forms by a first-order transition from the melt with a latent heat, we expect it to be more stable than a frozen-melt glass, whose thermodynamic properties approximate the undercooled liquid.

Are there other examples of q glasses? Can we define a q glass in a manner that helps us recognize q glasses and infer their properties? How are they to be distinguished from frozen-melt glasses? One definition arises from thermodynamics. The Al-Fe-Si q glass reported here was formed by a first-order transition from a melt. The consequences of the “formation by first-order transformation” definition include a lower energy, a greater stability, and a different ordering and composition compared to a frozen melt. Finding a lower energy structure would imply formation by first-order transitions.

Regarding this high degree of order with no translational and orientational order, how does the glass structure form at the growth front with the melt? Does the atomic surface of the q glass form the template for successive growth, or is there enough time for relaxation independent of a template? And finally, we need to understand why, during the growth of the q glass, the directional order that typifies crystals and quasicrystals is either lost or never established.

One possible explanation for the loss of orientational order is the presence of local frustration during growth. If incompatible packing configurations grow from the same seed cluster, local frustration would likely disrupt the long-range ordering. Such disordered packings of Mackay-based clusters in 2D have been observed using TEM in the Ti-Mn-Si system [14].

A more intriguing possibility consistent with the PDF results is that we have a realization of one of the many 3D ordered configurations of points that are neither periodic nor quasiperiodic [1]. The quasicrystalline phases taught us that stable atomic ordering does not require translational symmetry. If the q glass turns out to be fully ordered, then the requirement for finite rotational symmetry in an ordered solid would also prove incorrect.

The authors thank Frank Biancanello for alloy preparation, Alexander Shapiro for assisting with the SEM measurements, Maureen Williams for x-ray characterization and Kil-Won Moon for isothermal calorimetry. We thank Marjorie Senechal for useful discussions. The x-ray studies were conducted on beam lines 1-ID and 11-ID at the APS. The APS is an Office of Science User Facility operated for the U.S. Department of Energy (DOE) Office of Science by Argonne National Laboratory, and was supported by the U.S. DOE under Contract No. DE-AC02-06CH11357.

*Corresponding author.

gglong@aps.anl.gov

- [1] M. Senechal, in *Quasicrystals and Geometry* (Cambridge University Press, New York, 1995) Chap. 7.
- [2] J. W. Cahn and L. A. Bendersky, *Mater. Res. Soc. Symp. Proc.* **806**, MM2.7.1 (2004).
- [3] W. Mullins and R. Sekerka, *J. Appl. Phys.* **34**, 323 (1963).
- [4] T. Proffen and S. J. L. Billinge, *J. Appl. Crystallogr.* **32**, 572 (1999).
- [5] M. Cooper, *Acta Crystallogr.* **23**, 1106 (1967).
- [6] K. Sugiyama, N. Kaji, and K. Hiraga, *Acta Crystallogr. Sect. C* **54**, 445 (1998).
- [7] S. D. Shastri, K. Fezzaa, A. Mashayeki, W.-K. Lee, P. B. Fernandez, and P. L. Lee, *J. Synchrotron Radiat.* **9**, 317 (2002).
- [8] B. F. Toby, *Powder Diffr.* **21**, 67 (2006).
- [9] K. W. Chapman, P. J. Chupas, G. G. Long, L. Bendersky, L. E. Levine, F. Mompiou, J. K. Stalick, and J. W. Cahn (to be published).
- [10] L. C. Chen and F. Spaepen, *Mater. Sci. Eng. A* **133**, 342 (1991).
- [11] L. C. Chen and F. Spaepen, *Nature (London)* **336**, 366 (1988).
- [12] J. L. Robertson, S. C. Moss, and K. G. Kreider, *Phys. Rev. Lett.* **60**, 2062 (1988).
- [13] V. Hansen, B. Hauback, M. Sundberg, C. Rømming, and J. Gjønnes, *Acta Crystallogr. Sect. B* **54**, 351 (1998).
- [14] L. E. Levine, P. C. Gibbons, and A. M. Viano, *Philos. Mag. B* **70**, 11 (1994).